Accepted Manuscript

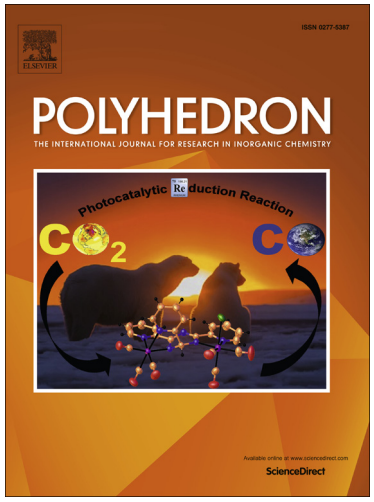

Synthesis and antiproliferative activity of ionic platinum(II) triphenylphosphino complexes

Daniela Belli Dell' Amico, Luca Labella, Fabio Marchetti, Simona Samaritani, Gustavo Alejandro Hernández-Fuentes, Aída Nelly García-Argáez, Lisa Dalla Via

PII: S0277-5387(16)30447-8
DOI: http://dx.doi.org/10.1016/j.poly.2016.09.019
Reference: POLY 12207

To appear in: *Polyhedron*

Received Date: 22 July 2016
Revised Date: 9 September 2016
Accepted Date: 10 September 2016

Please cite this article as: D.B. Dell' Amico, L. Labella, F. Marchetti, S. Samaritani, G.A. Hernández-Fuentes, A.N. García-Argáez, L. Dalla Via, Synthesis and antiproliferative activity of ionic platinum(II) triphenylphosphino complexes, *Polyhedron* (2016), doi: http://dx.doi.org/10.1016/j.poly.2016.09.019

Polyhedron

Synthesis and antiproliferative activity of ionic platinum(II) triphenylphosphino complexes

Daniela Belli Dell' Amico,[a] Luca Labella,[a] Fabio Marchetti,[a] Simona Samaritani[a,*]
Gustavo Alejandro Hernández-Fuentes,[b,d] Aída Nelly García-Argáez,[c,d] and Lisa Dalla Via[d]

[a] *Dipartimento di Chimica e Chimica Industriale, Università di Pisa, via Giuseppe Moruzzi 13, Pisa I-56124*

[b] *Facultad de Ciencias Químicas, Universidad de Colima, Kilómetro 9 Carretera Colima-Coquimatlán, Código Postal 28400, Coquimatlán, Colima, México*

[c] *Fondazione per la Biologia e la Medicina della Rigenerazione T.E.S.-Tissue Engineering and Signalling Onlus, Via F. Marzolo,13, 35131 Padova, Italy*

[d] *Dipartimento di Scienze del Farmaco, Università degli Studi di Padova, Via F. Marzolo 5, 35131 Padova, Italy*

Corresponding author: Simona Samaritani
tel. +39 050 2219 261
e.mail: simona.samaritani@unipi.it

Abstract: Ionic platinum(II) complexes $[PtCl(PPh_3)(L\wedge L)][BF_4]$ {L∧L = 2,2'-bipyridyl (**1**) 1,10-phenanthroline (**2**)} and $[PtCl(PPh_3)(L)_2][BF_4]$ {L = pyridine (**3**), dimethyl sulfoxide (**4**)} were synthesized by dehalogenation of *cis*-$[PtCl_2(PPh_3)(NCMe)]$, followed by reaction with the suitable ligand. Chelating nitrogen ligands L∧L afforded single products, which were structurally characterized. In the other cases mixtures of geometric (L = pyridine) and/or coordination (L = dimethyl sulfoxide) isomers were observed in solution. In these cases the structures of the less soluble isomers were obtained via single crystal X-ray diffraction. All the complexes were tested *in vitro* for their antiproliferative activity on three human tumor cell lines: MSTO-211H, HeLa and HepG2.

Keywords: platinum(II); triphenylphosphine; ionic complexes; chelating ligands; antiproliferative activity.

1. Introduction

Following the early discover of cisplatinum anticancer properties [1], hundreds of new platinum(II) complexes have been synthesized and tested *in vitro* for their antiproliferative activity. Among them, ionic, monofunctional complexes were originally disregarded as inactive [2], but have recently gained renewed interest as non-conventional anticancer agents displaying ranges of applicability and mechanisms of action other than classical agents [3]. The most studied

monofunctional ionic derivatives include [$PtClL_2L'$][X] complexes, where "L_2" represents a bidentate amine or two monodentate amine residues and L' is a N-heterocycle [3c,e-f,m], a sulfoxide [3i,k-l] or a thiourea derivative [3g], while fewer examples are described where monofunctional complexes contain P-coordinated ligands [4].

In the context of our studies concerning platinum (II) complexes containing triphenylphosphine [5], we have prepared four new ionic complexes characterized, besides PPh_3, by a chloride and, on the other two coordination sites, by a chelating N,N- coordinated ligand (**1**, **2**, Figure 1) or two non-chelating ligands (**3**, **4**, Figure 1). We report here the synthesis, the characterization and the antiproliferative activity of **1**-**4** against MSTO-211H (human biphasic mesothelioma), HeLa (human cervix adenocarcinoma) and HepG2 (human hepatocellular carcinoma) cell lines.

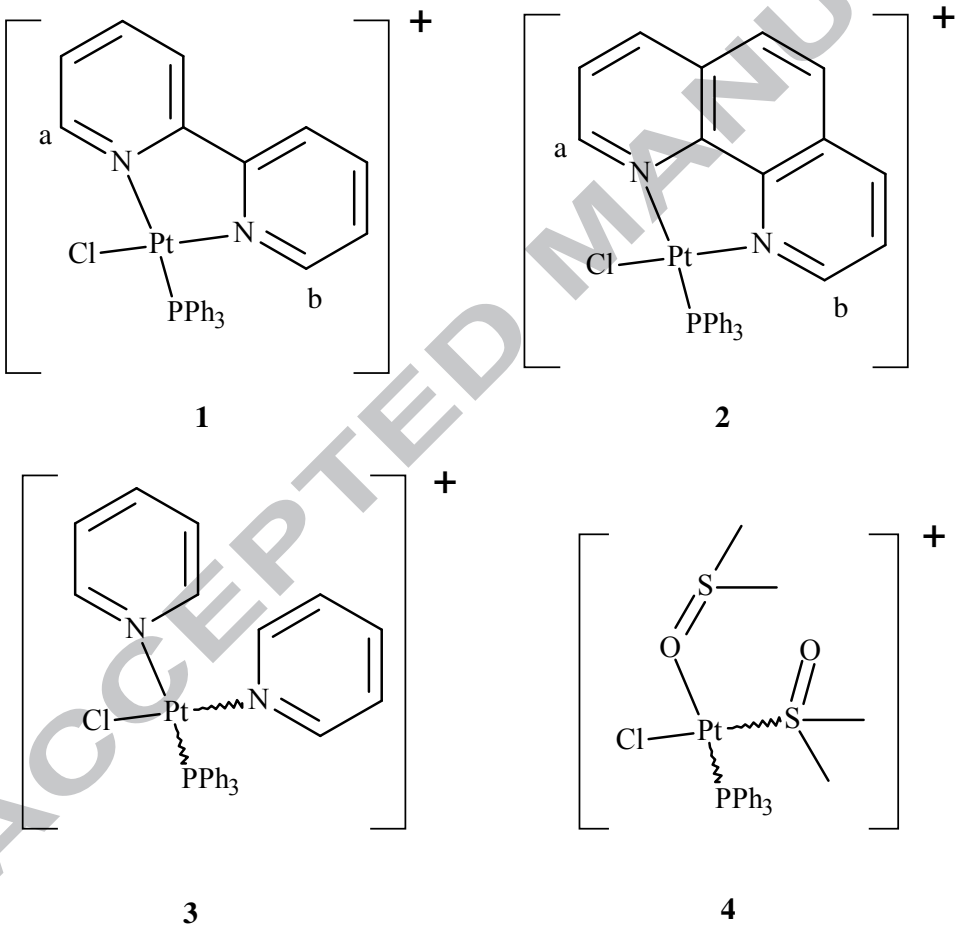

Figure 1. Structure of monocationic complexes **1**-**4**. Counterion was $[BF_4]^-$ for all complexes.

2. Experimental

2.1. Materials and general methods

All manipulations were performed under a dinitrogen atmosphere, if not otherwise stated. Solvents and liquid reagents were dried according to reported procedures [6]. ^{1}H-, ^{13}C-, ^{31}P-and ^{195}Pt-NMR spectra were recorded with a Bruker ''Avance DRX400'' spectrometer, in CD_3CN solution if not otherwise stated. Chemical shifts were measured in ppm (δ) from TMS by residual solvent peaks for ^{1}H- and ^{13}C-, from aqueous (D_2O) H_3PO_4 (85%) for ^{31}P- and from aqueous (D_2O) hexachloroplatinic acid for ^{195}Pt-NMR. A sealed capillary containing C_6D_6 was introduced in the NMR tube to lock the spectrometer to the deuterium signal when non-deuterated solvents were used. FTIR spectra in solid phase were recorded with a Perkin–Elmer ''Spectrum One'' spectrometer, equipped with an ATR accessory. Elemental analyses (C, H, N) were performed at Dipartimento di Scienze e Tecnologie Chimiche, Università di Udine. *Cis*-[$PtCl_2(PPh_3)(NCMe)$] was prepared according to a reported procedure [5f]. In the text the following abbreviations were used: 2,2'-bipyridyl (bipy); 1,10-phenanthroline (phen); pyridine (py).

*2.2. General procedure for the synthesis of ionic complexes **1**-**3**.*

A portion of *cis*-[$PtCl_2(PPh_3)(NCMe)$] (~ 0.5 mmol) was warmed (40 °C) and stirred in a mixture of MeCN and $MeNO_2$ (1/1 v/v) up to complete dissolution of the reagent. Solid $AgBF_4$ ([Ag]/[Pt] molar ratio = 1.2) was added under stirring and the flask was shielded from light. A colorless solid formed immediately and the suspension was stirred at room temperature for 1 h. A sample of the supernatant colorless solution was analyzed (^{31}P-NMR: 0.30, $^{1}J_{P\text{-}Pt}$ = 3748 Hz). The suspension was filtered on a short package of dry celite and the resulting colorless solution was treated with the suitable ligand ([L∧L]/[Pt] molar ratio = 1.0 for the chelating ligands and [py]/[Pt] molar ratio = 2.0 for py). The solution was monitored until complete conversion was obtained (^{31}P-NMR). Later on, it was concentrated *in vacuo* and Et_2O was added. Solid products were filtered, washed with two portions of Et_2O and dried *in vacuo* (10^{-2} mmHg). For each complex the isolated product % yield, the elemental analysis and the spectroscopic (IR and NMR) characterization are reported below.

*2.2.1 Cis-[$PtCl(PPh_3)(bipy)][BF_4$], **1**.*

50 % yield. *Anal.* Calcd. for $C_{28}H_{23}BClF_4N_2PPt$: C 45.7, H 3.2, N 3.8 %. Found: C 45.4, H 2.8, N 3.9 %. IR (ATR, cm^{-1}): 3086, 1606, 1451, 1432, 1315, 1276, 1243, 1174, 1098, 1054, 1046, 1033, 1024, 767, 752, 746; ^{1}H-NMR: 9.58 (m, 1H, $^{3}J_{H\text{-}Pt}$ = 36.0 Hz, Ha_{bipy}, Fig. 1), 8.45 (m, 4H,

H_{bipy}),7.97-7.87 (m, 8H, $2H_{bipy}$ + 6 H_{arom} phosphine), 7.65 (m, 3H, H_{arom} phosphine), 7.55 (m, 6H, H_{arom} phosphine), 7.07 (m, 1H, Hb_{bipy}, Fig. 1); ^{13}C-NMR: 157.9, 156.1, 152.3, 147.9, 142.4, 141.4, 135.0 (J_{C-P} = 10.9 Hz), 132.4, 129.0 (J_{C-P} = 11.5 Hz), 129.9, 127.7, 126.8 ($^1J_{C-P}$ = 64.7 Hz),124.6, 123.9; ^{31}P-NMR: 11.32 ($^1J_{P-Pt}$ = 3677 Hz); ^{195}Pt-NMR: -3541 ($^1J_{Pt-P}$ = 3677 Hz). A sample of solid was dissolved in $MeNO_2$ and crystallized by slow diffusion of diethyl ether vapors. Single crystals were selected for X-ray diffraction analysis.

*2.2.2. Cis-[PtCl(PPh$_3$)(phen)][BF$_4$], **2**.*

54 % yield. *Anal.* Calcd. for $C_{30}H_{23}BClF_4N_2PPt$: C 47.4, H 3.1, N 3.7 %. Found: C 47.2, H 2.7, N 3.8 %. IR (ATR, cm^{-1}): 3104, 3064, 1588, 1519, 1481, 1438, 1260, 1096, 1047, 1035, 845, 747; ^{1}H-NMR: 9.84 (m, 1H, Ha_{phen}, Fig. 1), 8.99 (m, 1H, H_{phen}), 8.80 (m, 1H, H_{phen}), 8.26 (m, 4H, H_{phen}), 7.93 (m, 6H, H_{arom} phosphine), 7.66 (m, 3H, H_{arom} phosphine), 7.55 (m, 6H, H_{arom} phosphine), 7.41 (m, 1H, Hb_{phen}, Fig. 1); ^{13}C-NMR: 158.1, 152.5, 148.8, 146.5, 141.3 (2C), 140.9 (2C), 135.2 (J_{C-P} = 10.8 Hz), 132.4 (J_{C-P} = 2.5 Hz), 129.0 (J_{C-P} = 11.7 Hz), 128.2, 128.0, 126.8 ($^1J_{C-P}$ = 64.7 Hz), 126.1, 126.0; ^{31}P-NMR: 11.09 ($^1J_{P-Pt}$ = 3690 Hz); ^{195}Pt-NMR: -3587 ($^1J_{Pt-P}$ = 3690 Hz). A sample of solid was dissolved in $MeNO_2$ and crystallized by slow diffusion of diethyl ether vapors. Single crystals were selected for X-ray diffraction analysis.

*2.2.3. Trans-[PtCl(PPh$_3$)(Py)$_2$][BF$_4$], **3**.*

60 % yield. *Anal.* Calcd. for $C_{28}H_{25}BClF_4N_2PPt$: C 45.6, H 3.4, N 3.8 %. Found: C 45.1, H 3.4, N 3.9%. IR (ATR, cm^{-1}): 3109, 3081, 3041, 1611, 1484, 1459, 1435, 1315, 1287, 1212, 1162, 1049, 1033, 996, 963, 881, 832, 768, 751, 710, 690; ^{1}H-NMR: 8.51 (m, 4H, $^3J_{H-Pt}$ = 38.4 Hz, C<u>H</u>N), 7.75 (m, 2H, C<u>H</u>CHCHN), 7.64 (m, 6H, H_{arom} phosphine), 7.55 (m, 3H, H_{arom} phosphine), 7.42 (m, 6H, H_{arom} phosphine), 7.20 (m, 4H, CHC<u>H</u>CHN); ^{13}C-NMR: 152.8, 139.8, 133.7 (J_{C-P} = 10.6 Hz), 132.1, 129.3 (J_{C-P} = 11.5 Hz), 126.8, 124.5 ($^1J_{C-P}$ = 63.2 Hz); ^{31}P-NMR: 5.20 ($^1J_{P-Pt}$ = 3824 Hz); ^{195}Pt-NMR: -3242 ($^1J_{Pt-P}$ = 3824 Hz). Single crystals were selected for X-ray diffraction analysis, which confirmed *trans* geometry.

*2.3. Synthesis of [PtCl(PPh$_3$)(SOMe$_2$)(OSMe$_2$)][BF$_4$], **4**.*

A sample (0.3035 g) of *cis*-[$PtCl_2$(PPh_3)(NCMe)] (0.533 mmol) was warmed (40 °C) and stirred in a mixture of DMSO and $MeNO_2$ (1/1 v/v) up to complete dissolution of the reagent. ^{31}P-NMR analysis on a sample of the solution showed the formation of *cis*-[$PtCl_2$(PPh_3)(DMSO)] (17.56, $^1J_{P-Pt}$ = 3770 Hz) [5c]. Solid $AgBF_4$ ([Ag]/[Pt] molar ratio = 1.2) was added under stirring and the flask was shielded from light. A colorless solid formed immediately and the suspension was stirred at

room temperature for 1 h. ^{31}P-NMR analysis on a sample of the supernatant liquid showed: 21.65 (65 %, $^{1}J_{P\text{-}Pt}$ = 3906 Hz), 9.16 (35 %, $^{1}J_{P\text{-}Pt}$ = 4058 Hz). The mixture was filtered on a short package of celite and the filtrate was concentrated up to half volume and treated with dry ethanol. Colorless crystals of [SP4-3]-**4** formed. A second crop of solid was obtained by precipitation with diethyl ether, in overall 34 % yield. *Anal.* Calcd. for $C_{22}H_{27}BClF_4S_2O_2PPt$: C 35.9, H 3.7%. Found: C 35.2, H 3.2%. IR (ATR, cm^{-1}): 3078, 3019, 2963, 1542, 1483, 1439, 1320, 1170, 1049, 1020, 899, 792, 760, 693; ^{1}H-NMR (CD_3NO_2, mixture of [SP4-3]-**4**/[SP4-2]-**4** in 70/30 molar ratio, signals of aliphatic hydrogens): [SP4-3]-**4**: 3.48 (s, 6H, $^{3}J_{H\text{-}Pt}$ = 25.6 Hz, PtS(O)(C$\underline{H}_3$)$_2$), 2.47 (s, 6H, PtOS(C$\underline{H}_3$)$_2$); [SP4-2]-**4**: 3.20 (s, 6H, $^{3}J_{H\text{-}Pt}$ = 18.0 Hz, PtS(O)(C$\underline{H}_3$)$_2$), 2.98 (bs, 6H, PtOS(C$\underline{H}_3$)$_2$); ^{13}C-NMR: (CD_3NO_2): [SP4-3]-**4**: 136.0 ($J_{C\text{-}P}$ = 10.8 Hz), 133.8, 130.2 ($J_{C\text{-}P}$ = 11.9 Hz), 127.3 ($^{1}J_{C\text{-}P}$ = 67.6 Hz), 47.5, 38.2; [SP4-2]-**4**: 135.9 ($J_{C\text{-}P}$ = 10.5 Hz), 133.7, 130.0 ($J_{C\text{-}P}$ = 12.0 Hz), 125.3 ($^{1}J_{C\text{-}P}$ = 65.3 Hz), 44.4, 37.1; ^{31}P-NMR: (CD_3NO_2): [SP4-3]-**4**: 19.09 ($^{1}J_{P\text{-}Pt}$ = 3883 Hz); [SP4-2]-**4**: 6.68 ($^{1}J_{P\text{-}Pt}$ = 4045 Hz);^{195}Pt-NMR (CD_3NO_2): [SP4-3]-**4**: -3626 ($^{1}J_{Pt\text{-}P}$ = 3883 Hz); [SP4-2]-**4**: -3832 ($^{1}J_{P\text{-}Pt}$ = 4045 Hz). Single crystals were selected for X-ray diffraction analysis, which confirmed the mode of coordination of DMSO residues and the geometry in [SP4-3]-**4**. A sample of these crystals was dissolved in CD_3NO_2 and analyzed: ^{31}P-NMR: 19.09 ($^{1}J_{P\text{-}Pt}$ = 3883 Hz), 6.68 ($^{1}J_{P\text{-}Pt}$ = 4045 Hz).

2.3. Inhibition growth assay

HepG2 (human hepatocellular carcinoma cells) and HeLa (human cervix adenocarcinoma cells) were grown in Dulbecco's Modified Eagle's Medium (Sigma Chemical Co.) and Nutrient Mixture F-12 [HAM] (Sigma Chemical Co.), respectively. MSTO-211H (human biphasic mesothelioma cells) were grown in RPMI 1640 (Sigma Chemical Co.) supplemented with 2.4 g/L HEPES and 0.11 g/L pyruvate sodium. 100 U/mL penicillin, 100 µg/mL streptomycin, 0.25 µg/mL amphotericin B (Sigma Chemical Co.) and 10% heat-inactivated fetal bovine serum (Invitrogen) were added to all media. The cells were cultured at 37°C in a moist atmosphere of 5% carbon dioxide in air. Cells (3 x 10^4) were seeded into each well of a 24-well cell culture plate. After incubation for 24 h, 20 µM concentration of the test agents was added to complete medium. The cells were then incubated in standard conditions for a further 72 h. Stock solutions of new complexes were made in dimethyl sulfoxide at 20 mM concentration and then diluted with complete medium in such way that the final amount of solvent did not exceed 0.5%. A trypan blue assay was performed to determine cell viability. Cytotoxicity data were expressed as percentage of viability with respect to control cultures.

2.4. X-ray structure determination

The X-ray diffraction experiments were carried out at room temperature by means of a Bruker Smart Breeze CCD diffractometer operating with graphite-monochromated Mo-K_α radiation for samples **2**, **3** and **4** and a Oxford Xcalibur3 diffractometer operating with Cu-K_α radiation for sample **1**. The samples were sealed in glass capillaries and their lattice parameters were evaluated as a preliminary step to the crystallographic study. The values obtained are reported in Table 1. On the basis of those results the intensity data collections were done up to the limits mentioned in the table. The intensities were corrected for Lorentz and polarisation effects and for absorption by means of a multi-scan method [7] for **2**, **3** and **4** and by an analytical method based on the crystal shape [8] for **1**. The structure solutions were obtained by the automatic direct methods contained in SHELX97 programme [9]. The abnormal anisotropy in the displacement parameters of fluorine atoms observed after the first refinement cycles either in **2** or in **3** and in **4** was considered as the result of disorder in the BF_4^- orientation. So the anions of those compounds were refined as distributed in two limit positions. For what concerns the structure of compound **4**, which contains two dimethylsulfoxide ligands bonded in two different ways, the abnormal anisotropy was present also in displacement parameters of the chlorine ligand and in some atoms of the O-connected dimethylsulfoxide. This feature, together with the presence of residual electron density peaks around the same dimethylsulfoxide, suggested us that further disorder was present also in these moieties of the cation. So both the chlorine and the O-connected dimethylsulfoxide ligand were introduced in this model as distributed in two limit positions. After the introduction of hydrogen atoms in calculated positions all the heavy atoms were refined with anisotropic thermal parameters till the reliability factors listed in Table 1.

In addition to the aforementioned software, other control calculations and preparation of publication material were performed with the programs contained in the suite WINGX [10].

Table 1. Crystal data and structure refinements

	1	**2**	**3**·0.5(acetonitryl)	**4**
Formula	$C_{28}H_{23}BClF_4N_2PPt$	$C_{30}H_{23}BClF_4N_2PPt$	$C_{29}H_{26.50}BClF_4N_{2.50}PPt$	$C_{22}H_{27}BClF_4O_2PPtS_2$
Fw ($g \cdot mol^{-1}$)	735.80	759.82	758.35	735.87
λ (Å)	1.54184	0.71073	0.71073	0.71073
Crystal system	Monoclinic	Monoclinic	Monoclinic	Monoclinic
Space group	$P2_1/c$	$P2_1/c$	$C2/c$	$P2_1/c$
a (Å)	9.82764(10)	10.4093(4)	29.014(2)	13.0960(3)
b (Å)	9.66342(10)	28.9096(11)	10.0688(8)	11.3103(4)
c (Å)	27.8911(3)	9.9297(4)	20.4056(17)	18.7516(5)
β (°)	90.1149(10)	114.589(2)	99.317(3)	92.068(2)
V ($Å^3$)	2648.77(5)	2717.15(19)	5882.6(8)	2775.67(14)
Z	4	4	8	4
ρ_{calc} ($Mg \cdot m^{-3}$)	1.845	1.857	1.713	1.761
μ (mm^{-1})	11.844	5.373	4.964	5.404

θ range (°)	4.499 - 72.370	3.092 - 32.426	2.941 - 35.972	2.174 - 26.948
Data collected	15009	34268	40943	22193
Independent reflections	4949	9604	12193	5976
R_{int}	0.0419	0.0496	0.0204	0.0480
Restraints/Parameters	0 / 343	0 / 331	0 / 307	106 / 401
Goodness-of-fit (GOF) on F^2	1.011	0.942	1.020	1.056
R_1; wR_2 [$I > 2\sigma(I)$]	0.0328; 0.0747	0.0468; 0.0947	0.0386; 0.1141	0.0434; 0.0967
R_1; wR_2 [all data]	0.0458; 0.0810	0.0896; 0.1101	0.0653; 0.1331	0.0843; 0.1151
Res. dens. (e·Å^{-3})	0.992; −1.296	1.362; −0.836	1.804; −3.033	1.594; −0.727

3. Results and discussion

3.1. Syntheses and characterizations.

The preparation of complexes **1**-**4** was carried out starting from *cis*-[$PtCl_2(PPh_3)(NCMe)$] [5f], according to the synthetic sequence depicted in Scheme 1. The syntheses were conveniently followed by ^{31}P-NMR spectroscopy.

Dechlorination of the precursor by $AgBF_4$ was efficiently achieved at room temperature, in $MeNO_2$/MeCN mixture and afforded *cis*-[$PtCl(PPh_3)(NCMe)_2$][BF_4] as single intermediate (Scheme 1, ***A***), as shown by the single signal observed in the ^{31}P-NMR spectrum (0.30, $^1J_{P\text{-}Pt}$ = 3748 Hz). This intermediate was not isolated, but *cis* geometry can be assumed on the basis of the strong *trans* effect exerted by PPh_3 ligand. Slow, partial isomerization to *trans* isomer was observed in solution, with the appearance of a new signal (5.04, $^1J_{P\text{-}Pt}$ = 3748 Hz) in about 30% amount, after 24h. Noteworthy, at room temperature, the second chloride is not removed from the platinum coordination sphere, even using a slight excess of $AgBF_4$.

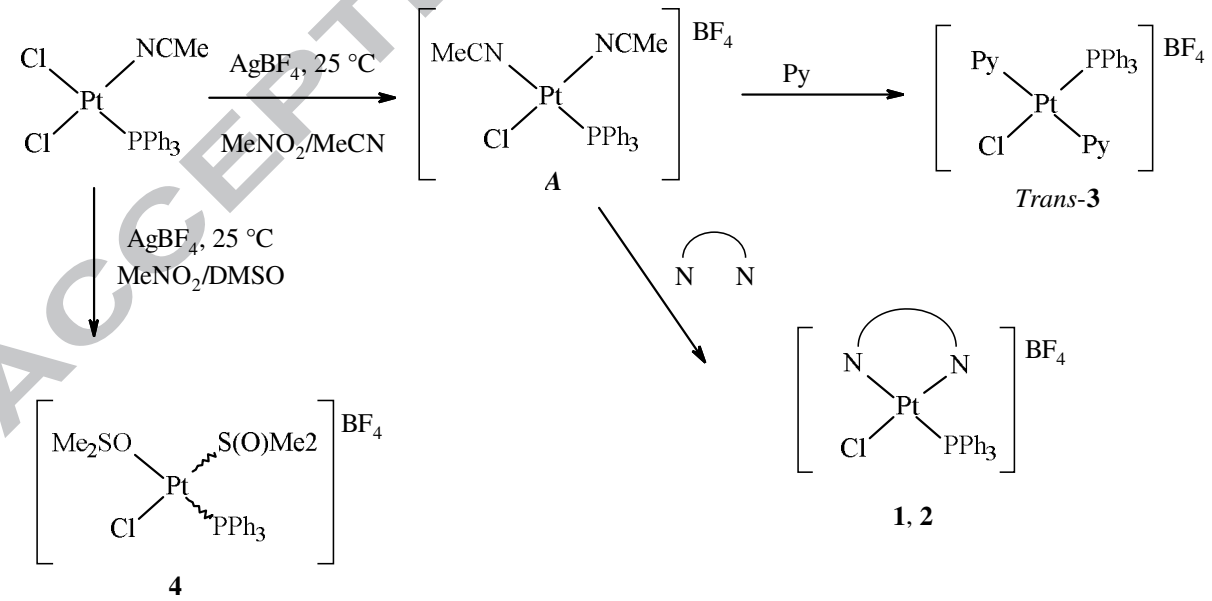

Scheme 1. Synthesis of **1**-**4**.

After removal of solid AgCl, the addition of equimolar amounts of chelating ligands 2,2'-bipyridine or 1,10-phenanthroline afforded smoothly complexes **1** and **2**. Both compounds, as expected for

symmetrical, chelating ligands, showed a single signal with satellites in the ^{31}P-NMR spectrum and a single doublet in the ^{195}Pt-NMR spectrum. They were recovered in good isolated yield, after concentration of the mixture and addition of diethylether. The elemental analyses, IR (ATR) spectroscopy and the ^{1}H- and ^{13}C-NMR characterization in solution were in agreement with the proposed structures. It is worth to mention that in the ^{1}H-NMR spectra of complexes **1** and **2** non-equivalent hydrogen atoms a and b (Figure 1) afforded two well separated signals, that were assigned by comparison with analogous triphenylphosphine complexes bearing *cis* and/or *trans* N-heteroaromatic ligands [11]. Both **1** and **2** were crystallized by slow diffusion of diethylether vapors into acetonitrile solutions and the structures were determined by X-ray diffraction.

The treatment of intermediate ***A*** with pyridine (2.2 molar equivalents) afforded a mixture of two products, as shown by ^{31}P-NMR analysis. The kinetic product *cis*-**3** (4.28, $^{1}J_{P\text{-}Pt}$ = 3568 Hz) was initially observed as the main component of the mixture, together with *trans*-**3** (6.46, $^{1}J_{P\text{-}Pt}$ = 3826 Hz). After 72h, anyway, *trans*-**3** was the main product in solution (80 %) and it was recovered pure after precipitation by diethylether. Its stereochemistry was checked by X-ray diffraction on a single crystal. Full NMR characterization (^{1}H-, ^{31}P-, ^{13}C- and ^{195}Pt-) of *trans*-**3** was carried out in CD_3CN, where the complex isomerizes very slowly. As expected, the four equivalent hydrogen atoms closest to the coordinated nitrogen atoms of pyridine rings, afforded a single, well separated ^{1}H-NMR multiplet with satellites ($^{3}J_{H\text{-}Pt}$ = 38.4 Hz).

The addition of dimethylsulfoxide (2.2 molar equivalents) to intermediate ***A*** did not cause any variation in the solution, showing thus a competition between DMSO and acetonitrile for coordination to platinum(II). Even when most of excess MeCN was eliminated, ^{31}P-NMR spectrum of the reaction mixture showed signals ascribable to species still containing coordinated acetonitrile. In a second experiment, thus, reaction was carried out in $MeNO_2$/DMSO (Scheme 1, preparation of **4**). Dissolution of *cis*-[$PtCl_2(PPh_3)(NCMe)$] in the used solvents caused its complete conversion into *cis*-[$PtCl_2(PPh_3)(SOMe_2)$] [5c], as shown by the appearance of a single signal in the ^{31}P-NMR spectrum (17.56, $^{1}J_{P\text{-}Pt}$ = 3770 Hz). After addition of $AgBF_4$ and elimination of solid AgCl, two products were observed in the solution [^{31}P-NMR: 21.65 (65 %, $^{1}J_{P\text{-}Pt}$ = 3906 Hz), 9.16 (35 %, $^{1}J_{P\text{-}Pt}$ = 4058 Hz)]. Crystals suitable for X-ray diffraction were obtained upon addition of dry ethanol and were identified as [SP4-3]-**4**, where two DMSO molecules are coordinated to platinum in mutual *trans* position, one by S- and the other by O- atoms. Although sulfoxides generally prefer S-coordination to platinum [12], examples of O-coordination are described [12,13]. IR (ATR) spectroscopic analysis was carried out on a sample of the crystals, where two bands at 1170 and 899 cm^{-1} were attributed to S–O stretching vibrations in S-coordinated and O-coordinated DMSO respectively, in agreement with literature data [12,13d]. A freshly prepared solution of the crystals

in CD_3NO_2 afforded (^{31}P-NMR) the previously observed two signals, with minimal variations due to the solvent change. This behavior showed the presence, in solution, of a rapid equilibrium involving [SP4-3]-**4** and another species, which was identified as [SP4-2]-**4** on the basis of ^{1}H- and ^{13}C- NMR spectra carried out on the solution (Scheme 2). The portion of ^{1}H-NMR spectrum where signals of DMSO residues were observed is reported in Figure 2. For each isomer, DMSO methyl groups are not equivalent (singlets *a*, *a'* for the main isomer and singlets *b*, *b'* for the other one). For signals *a* and *b* $^{3}J_{H\text{-}Pt}$ coupling constants of 25 and 18 Hz respectively could be measured. This feature, together with the chemical shifts observed (3.48 and 3.19 ppm), is typical of S-coordinated DMSO in platinum complexes [12c,13d,14]. On the other hand, signals *a'* and *b'* were observed at 2.47 and 2.99 ppm as singlets, without any measurable H-Pt coupling constants, in agreement with data described for O-coordinated DMSO ligands [12c,13d,14]. An appreciable broadening was observed for signal *b'* (Figure 2). It seems reasonable to attribute this resonance to O-coordinated DMSO of [SP4-2]-**4**, due to the strong *trans* effect exerted by PPh_3.

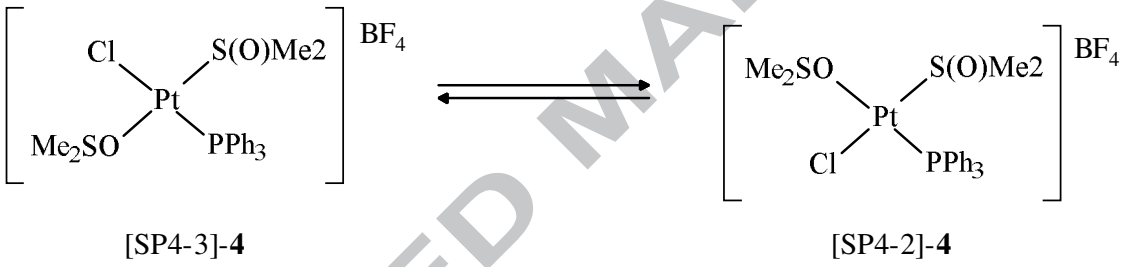

[SP4-3]-**4** [SP4-2]-**4**

Scheme 2. Equilibrium between [SP4-3]-**4** and [SP4-2]-**4** in CD_3NO_2 solution.

The presence of a S-coordinated and an O-coordinated DMSO ligands in both isomers [SP4-3]-**4** and [SP4-2]-**4** was confirmed by ^{13}C-NMR spectrum in CD_3NO_2. Non-equivalent methyl groups of main isomer afforded signals at 47.5 and 38.2, while for the other complex signals at 44.4 and 37.1 ppm were observed, in agreement with literature data [15] reporting high-field or low-field shifts with respect to free DMSO in case of O- or S-coordination respectively.

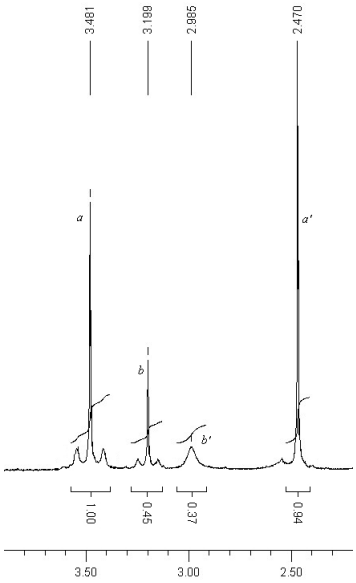

Figure 2. ^{1}H-NMR signals of methyl hydrogen atoms in [SP4-3]-**4**/[SP4-2]-**4** mixture

Complexes **1**-**4** were stable in DMSO solution, as checked by ^{31}P-NMR spectroscopy.

3.2 Structural determinations

Selected bond lengths and angles for complexes **1**-**3** are reported in Table 2, while the views of molecular structures for the same cations are represented in Figure 3. In all cases, the coordination around platinum(II) is square planar, with small deviations from ideality.

Table 2. Selected bond lenghts (Å) and angles (°) in the structures of **1**-**3**.

	1	**2**	**3**·0.5(CH_3CN)
Pt(1)–Cl(1)	2.2727(12)	2.2755(14)	2.3427(10)
Pt(1)–P(1)	2.2542(12)	2.2556(12)	2.2481(10)
Pt(1)–N(1)	2.054(4)	2.052(4)	2.015(3)
Pt(1)–N(2)	2.087(4)	2.090(4)	2.029(4)
P(1)–Pt(1)–Cl(1)	89.43(5)	90.66(5)	176.60(4)
P(1)–Pt(1)–N(1)	98.33(13)	97.88(12)	93.42(10)
P(1)–Pt(1)–N(2)	176.20(12)	177.23(12)	90.07(10)
Cl(1)–Pt(1)–N(1)	172.04(13)	171.46(12)	88.12(10)
Cl(1)–Pt(1)–N(2)	92.75(13)	91.26(13)	88.48(10)
N(1)–Pt(1)–N(2)	79.60(18)	80.21(18)	176.16(14)

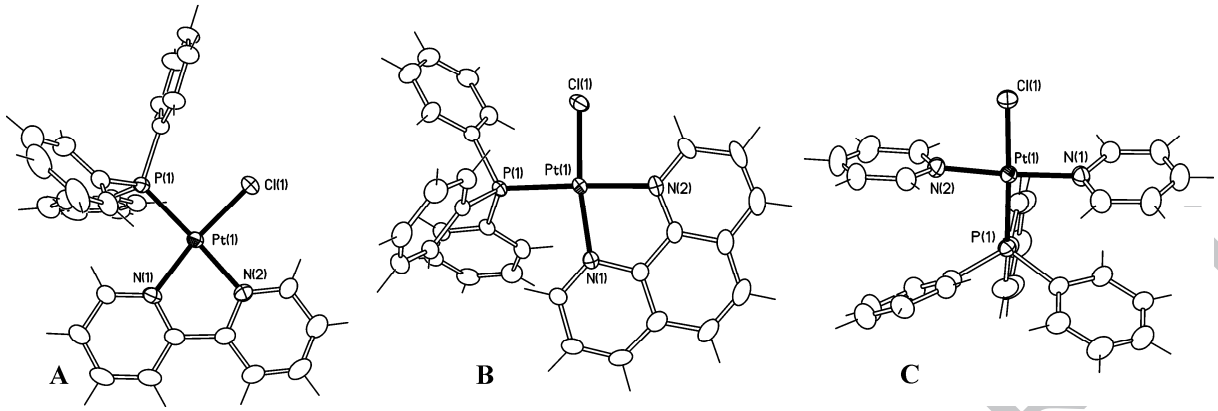

Figure 3. View of the molecular structure of cations $[Pt(PPh_3)BipyCl]^+$ as found in the crystal of **1** (**A**), $[Pt(PPh)_3PhenCl]^+$ as found in the crystal of **2** (**B**) and $[Pt(PPh)_3Py_2Cl]^+$ as found in the crystal of **3** (**C**).

Bond lengths and angles in complexes **1** and **2** are very similar between themselves, with Pt–N(2) bond distance slightly longer than Pt–N(1) one in both cases. This feature is probably related to the trans influence exerted by the PPh_3 group and is in agreement with an analogous cationic complex bearing PPh_3 and 1,10-phenanthroline-5,6-dione residues [16]. In the case of complex **2**, π–π stacking interactions between phenanthroline rings of contiguous molecules was observed, at variance with the aforementioned structure [16], where steric hindrance of bulky PPh_3 seems to prevent this intermolecular interaction. In our case, planar phenanthroline or dipyridine ligands of two contiguous molecules are parallel and staggered (Figure 4), with the distance between the parallel plans only slightly higher than in graphite [17] (3.42 -3.54 Å *vs.* 3.35Å).

In complex **3**, Pt–Cl bond distance is longer than in complexes **1** and **2**, as expected, due to the presence of PPh_3 residue in the *trans* position.

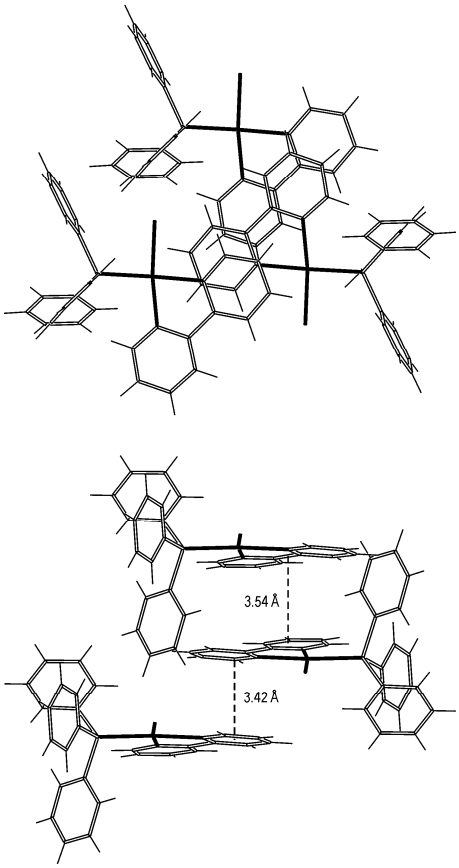

Figure 4. Intermolecular stacking interactions in *cis*-[Pt(PPh$_3$)(phen)Cl]$^+$

The most significant geometric parameters for [SP4-3]-**4** are reported in Table 3. The coordination around platinum(II) is square planar, with the two DMSO units in mutual *trans* position, one S- and the other O-coordinated. Chloride and O-DMSO ligands are disordered and, in the model, have been refined as distributed in two limit positions. In the view of the molecular structure of [SP4-3]-**4** (Figure 5), only the most populated limit positions have been represented.

Table 3. Selected bond lenghts (Å) and angles (°) for [SP4-3]-**4**

Pt(1)–Cl(1A)	2.322(8)	Pt(1)–S(1)	2.2011(16)
Pt(1)–P(1)	2.2684(15)	Pt(1)–O(2A)	2.102(11)
S(1)–Pt(1)–Cl(1A)	90.6(3)	P(1)–Pt(1)–S(1)	92.32(6)
O(2A)–Pt(1)–Cl(1A)	91.2(4)	O(2A)–Pt(1)–S(1)	177.4(3)
P(1)–Pt(1)–Cl(1A)	168.0(10)	O(2A)–Pt(1)–P(1)	85.6(3)

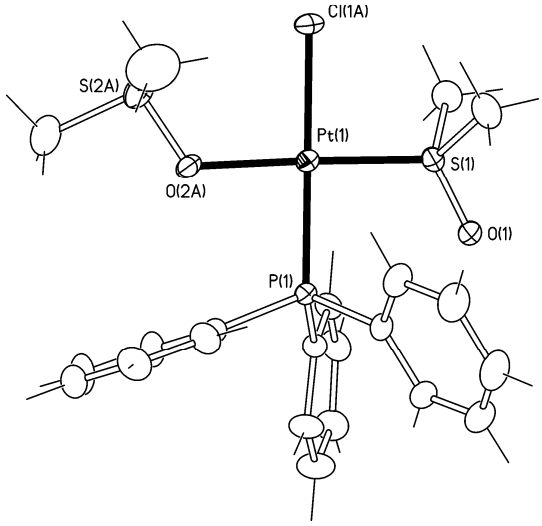

Figure 5. View of the molecular structure of cation $[PtCl(PPh)_3(DMSO)_2]^+$ as found in the crystal of [SP4-3]-**4**. Chlorine and one dimethylsulfoxide ligand are disordered. Thermal ellipsoids are at 20% probability.

Analogous ionic complexes of Ru(II) [18], Rh(III) [19], Pd(II) [20] and Pt(II) [13c] are described where at least two DMSO units are coordinated by sulphur and oxygen atoms. Our derivative can be compared with *cis*-$[Pt(SOMe_2)_2(OSMe_2)_2][CF_3SO_3]_2$ [13c], where coordination around platinum(II) is again square planar with only slight deviations and O- and S-coordinated DMSO ligands are in mutual *trans* positions. As for bond lengths, a longer Pt–O bond distance was observed in [SP4-3]-**4** than in the aforementioned [13c] homoleptic compound (2.089 *vs.* a mean value of 2.045 Å), while S–Pt bond is shorter (2.202 *vs.* 2.207 Å). Finally, S–O bond distances in [SP4-3]-**4** are shorter than in the other complex (1.430 *vs.* 1.453 Å for S-coordinated ligand and 1.510 *vs.* 1.545 Å for the O-coordinated one).

3.3 Inhibition growth assay

The cytotoxic effect of the new complexes **1**-**4** was evaluated on three human tumor cell lines, MSTO-211H (human biphasic mesothelioma), HeLa (human cervix adenocarcinoma) and HepG2 (human hepatocellular carcinoma). The results have been expressed as percentage of cell viability with respect to control cultures and have been reported in Table 4.

Table 4. Cell viability in the presence of platinum complex 1-4 at 20 µM concentration.

Complex	Cell lines [a,b] (viability %)		
	MSTO-211H	HeLa	HepG2
1	63.81	90.15	81.42
2	29.52	89.37	95.35

3	70.48	97.30	95.35
4	86.67	100	99.45

[a] Values are the mean of three independent experiments.
[b] Results are expressed as percentage of viability with respect to control cultures.

All synthesized complexes exert a weak cytotoxicity on the cell lines taken into account, nevertheless, the MSTO-211H cells appear the most sensitive, showing the lower viability percentage values for all considered complexes, with respect to both HeLa and HepG2. In particular, on mesothelioma cells the cell viability decreases from 86.67% in the presence of complex **4** to 29.52% when incubated with complex **2**. Interestingly, in this cell line the observed cytotoxic effect appears dependent on the increase in steric hindrance of the substituent or of the chelating group coordinating the metal. This behavior appears confirmed also for HeLa cells, while for HepG2, likely due to the very low antiproliferative effect, none relationship can be highlighted.

4. Conclusions

Ionic platinum complexes containing PPh_3 can be conveniently prepared by dechlorination of *cis*-$[PtCl_2(PPh_3)(NCMe)]$ [5f] by a slight excess of $AgBF_4$ at room temperature, followed by the suitable nucleophile. While the use of symmetric chelating bidentate ligands (bipy and phen) affords single products, with monodentate ligands mixtures of geometric (L = Py) and/or coordination (L = DMSO) isomers are observed in solution. In both cases studied, anyway, a single isomer was isolated and structurally characterized. The structure of DMSO complex [SP4-3]-$[PtCl(PPh_3)(SOMe_2)(OSMe_2)]^+$ is particularly interesting for the presence of two DMSO residues bonded to platinum by sulphur and oxygen atoms and in mutual *trans* position. To the best of our knowledge there is only another example of this kind in the literature [13c]. The DMSO complex showed a dynamic behavior in solution, where ^{1}H- and ^{31}P-NMR spectroscopy allowed to observe the presence of an equilibrium between [SP4-3]- and [SP4-2]-**4** isomers. The constant of the equilibrium (1), assessed by the integration of ^{1}H-NMR signals of methyl groups, is about 0.4 (CD_3NO_2, 25 °C).

$$\text{[SP4-3]-}\mathbf{4} \underset{}{\overset{K}{\rightleftharpoons}} \text{[SP4-2]-}\mathbf{4} \qquad (1)$$

The cytotoxic effect exerted by complexes **1**-**4** on MSTO-211H (human biphasic mesothelioma), HeLa (human cervix adenocarcinoma) and HepG2 (human hepatocellular carcinoma) cell lines was

generally low. Anyway, the highest activity was exerted by phenanthroline complex **2** against the most sensitive MSTO-211H cell line. This result suggest that the presence of chelating, sterically hindered bidentate ligands could enhance the antiproliferative activity.

Acknowledgements. The authors thank the Università di Pisa for financial support (Fondi di Ateneo 2015). S. Samaritani is grateful to the financial support provided by Università di Pisa—Progetti di Ricerca di Ateneo 2015—'Sintesi e studio delle proprietà di composti di metalli di transizione come agenti Antitumorali' (PRA_2015_0055). L.D.V. thanks the financial supports of the Italian Ministry for University and Research (MIUR) and Consorzio Interuniversitario di Ricerca in Chimica dei Metalli nei Sistemi Biologici (CIRCMSB).

Appendix A. Supplementary data

CCDC 1495239-1495242 contain the supplementary crystallographic data for the derivatives **1**, **2**, *trans*-**3**$^{\cdot}$and [SP4-3]-**4**$^{\cdot}$. These data can be obtained free of charge from The Cambridge Crystallographic Data Centre via www.ccdc.cam.ac.uk/data_request/cif

1 a) B. Rosenberg, L. VanCamp, T. Krigas, Nature, 205 (1965), 698;
b) B. Rosenberg, L. VanCamp, J. E. Trosko, V. H. Mansour, Nature, 222(1969), 385.

2 a) M. J. Cleare, J. D. Hoeschele, Plat. Met. Rev., 17 (1973), 2;
b) J.-P. Macquet, J.-L. Butour, J. Natl. Cancer Inst., 70 (1983), 899.

3 a) T. C. Johnstone, K. Suntharalingam, S. J. Lippard, Chem. Rev., 116 (2016), 3436;
b) J. J. Wilson, S. J. Lippard, Chem. Rev., 114 (2014), 4470;
c) T. C. Johnstone, J. J. Wilson, S. J. Lippard, Inorg. Chem., 52 (2013), 12234;
d) K. S. Lovejoy, S. J. Lippard, Dalton Trans., 2009, 10651;
e) B. Wang, Z. Wang, F. Ai, W. K. Tang, G. Zhu, J. Inorg. Biochem., 142 (2015), 118;
f) G. Y. Park, J. J. Wilson, Y. Song, S. J. Lippard, Proc. Natl. Acad. Sci., 109 (2012), 11987;
g) J. Suryadi, U. Bierbach, Chem. Europ. J., 18 (2012), 12926;
h) H. Baruah, C. G. Barry, U. Bierbach, Curr. Top. Med. Chem., 4 (2004), 1537;
i) L. Fuks, K. Samochocka, R. Anulewicz-Ostrowska, M. Kruszewski, W. Priebe, W. Lewandowski, Europ. J. Med. Chem., 38 (2003), 775;
j) S. Wu, X. Wang, C. Zhu, Y. Song, J. Wang, Y. Lia, Z. Guo, Dalton Trans., 40 (2011), 10376;
k) J. Landi, M. P. Hackerb, N. Farrell, Inorg. Chim. Acta, 202 (1992), 79;
l) N. Farrell, D. M. Kiley, W. Schmidt, M. P. Hacker, Inorg. Chem., 29 (1990), 397;
m) L. S. Hollis, A. R. Amundsen, E. W. Stern, J. Med. Chem., 32 (1989), 128.

4 a) W. Villarreal, L. Colina-Vegas, C. Rodrigues de Oliveira, J. C. Tenorio, J. Ellena, F. C. Gozzo, M. R. Cominetti, A. G. Ferreira, M. A. Barbosa Ferreira, M. Navarro, A. A. Batista, Inorg. Chem., 54 (2015), 11709;
b) A. Habtemariam, J. A. Parkinson, N. Margiotta, T. W. Hambley, S. Parsons, P. J. Sadler, J. Chem. Soc., Dalton Trans., 2001, 362;
c) K. Neplechová, J. Kašpàrková, O. Vrána, O. Nováková, A. Habtemariam, B. Watchman, P. J. Sadler, V. Brabec, Molecul. Pharm., 56 (1999), 20;
d) N. Margiotta, A. Habtemariam, P. J. Sadler, Angew. Chem. Int. Ed. Eng., 36 (1997), 1185;
e) A. Habtemariam, P. J. Sadler, Chem. Commun., 1996, 1785.

5 a) L. Dalla Via, A. N. García-Argáez, E. Agostinelli, D. Belli Dell'Amico, L. Labella, S. Samaritani, Bioorg. Med. Chem. 24 (2016), 2929;
b) L. Nierzwicki, M. Wieczor, V. Censi, M. Baginski, L. Calucci, S. Samaritani, J. Czub, C. Forte, Phys. Chem. Chem. Phys., 17 (2015), 1458;
c) D. Belli Dell' Amico, L. Dalla Via, A. N. García-Argáez, L. Labella, F. Marchetti, S, Samaritani, Polyhedron, 85 (2015), 685;
d) L. Dalla Via, A. N. García-Argáez, A. Adami, S. Grancara, P. Martinis, A. Toninello, D. Belli Dell'Amico, L. Labella, S. Samaritani, Bioorg. Med. Chem., 21 (2013), 6965;
e) D. Belli Dell'Amico, C. Broglia, L. Labella, F. Marchetti, D. Mendola, S. Samaritani, Inorg. Chim. Acta, 395 (2013), 181;
f) D. Belli Dell'Amico, L. Labella, F. Marchetti, S. Samaritani, Dalton Trans., 41 (2012), 1389.

6 W. L. F. Armarego, D. D. Perrin, Purification of Laboratory Chemicals, Butterworth-Heinemann, 1996.

7 G. M. Sheldrick, *SADABS*, Program for empirical absorption correction, University of Göttingen, Germany, **1996**.

8 *CrysAlisPro*, Agilent Technologies Ltd, Yarnton, Oxfordshire, England, 2014.

9 SHELX97 - Programs for Crystal Structure Analysis (Release 97-2). Sheldrick, G.M., Institüt für Anorganische Chemie der Universität, Tammanstrasse 4, D-3400 Göttingen, Germany, 1998.

10 L. J. Farrugia, J. Appl. Crystallogr., 32 (1999), 837.

11 a) D. Belli Dell' Amico, L. Bellucci, L. Labella, F. Marchetti, S. Samaritani, Polyhedron, in press.

12 a) M. Calligaris, Coord. Chem. Rev., 248 (2004), 351;
b) M. Calligaris, O. Carugo, Coord. Chem. Rev., 153 (1996), 83;
c) G. A. Davies, Adv. Inorg. Chem. Radiochem., 24 (1981), 115.

13 a) E. E. Drinkel, L. Wu, A. Linden, R. Dorta, Organometallics, 33 (2014), 627;
b) G. Annibale, L. Cattalini, V. Bertolasi, V. Ferretti, G. Gilli, M. L. Tobe, J. Chem. Soc. Dalton Trans., 1989, 1265;

c) L. A. Elding, Å. Oskarsson, Inorg. Chim. Acta, 130 (1987), 209;
d) J. A. Davies, F. R. Hartley, S. G. Murray, J. Chem. Soc. Dalton Trans., 1979, 1705.
14 P. Bergamini, L. Marvelli, V. Ferretti, C. Gemmo, R. Gambari, Y. Hushcha, I. Lampronti, Dalton Trans., 45 (2016), 10752.
15 J. D. Fothenngon, J. Chem. Res., 3 (1986), 82.
16 R. Okamura, T. Fujihara, T. Wada, K. Tanaka, Bull. Chem. Soc. Jpn., 79 (2006), 106.
17 L. A. Girifalco, R. A. Lad, J. Chem. Phys., 25 (1956), 693.
18 a) A. R. Davies, F. W. B. Einstein, N. P. Farrell, B. R. James, R. S. Mc Millan, Inorg. Chem., 17 (1978), 1965;
b) I. Bratsos, C. Simonin, E. Zangrando, T. Gianferrara, A. Bergamo, E. Alessio, Dalton Trans., 40 (2011), 9533.
19 a) A. Abbasi, M. Yu. Skripkin, L. Eriksson, N. Torapava, Dalton Trans., 40 (2011), 1111;
b) R. Dorta, H. Rozenberg, D. Milstein, Chem. Commun., 2002, 710.
20 B. F. G. Johnson, J. Puga, P. R. Raithby, Acta Cryst., B37 (1981), 953.

Synopsis

Synthesis and antiproliferative activity of ionic platinum(II) triphenylphosphino complexes

by Daniela Belli Dell' Amico, Luca Labella, Fabio Marchetti, Simona Samaritani, Gustavo Alejandro Hernández Fuentes, Aída Nelly García-Argáez, and Lisa Dalla Via

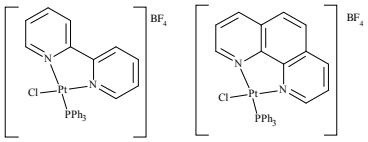

1

2

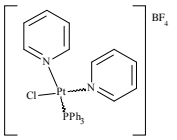

3

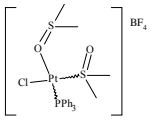

4

Dehalogenation of *cis*-[$PtCl_2(PPh_3)(NCMe)$], followed by ligand substitution afforded ionic complexes [$PtCl(PPh_3)(L\wedge L)][BF_4$] {L^L = 2,2'-bipyridyl (**1**) 1,10-phenanthroline (**2**)} and [$PtCl(PPh_3)(L)_2][BF_4$] {L = pyridine (**3**), dimethyl sulfoxide (**4**)}. The complexes were characterized by X-ray diffraction and spectroscopic techniques. Antiproliferative activity against MSTO-211H, HeLa and HepG2 tumor cell lines was evaluated *in vitro*.